

This is the Submitted version (post-print) of the following paper: alginate/human elastin-like polypeptide composite films with antioxidant properties for potential wound healing application by Bergonzi et al. published on International Journal of Biological Macromolecules Volume 164, 1 December 2020, Pages 586-596, DOI: <https://doi.org/10.1016/j.ijbiomac.2020.07.084>. The final published version is available on the publisher website

# ALGINATE/HUMAN ELASTIN-LIKE POLYPEPTIDE COMPOSITE FILMS WITH ANTIOXIDANT PROPERTIES FOR POTENTIAL WOUND HEALING APPLICATION

Carlo Bergonzi<sup>a,1</sup>, Giovanna Gomez d'Ayala<sup>b,1</sup>, Lisa Elviri<sup>a</sup>, Paola Laurienzo<sup>b</sup>,  
Antonella Bandiera<sup>c</sup>, Ovidio Catanzano<sup>c,\*</sup>

*a Food and Drug Department, University of Parma, Parco Area delle Scienze 27/A, 43124 Parma, Italy*

*b Institute for Polymers, Composites and Biomaterials (IPCB) – CNR, Via Campi Flegrei 34, 80078  
Pozzuoli (NA), Italy*

*c Department of Life Sciences, University of Trieste, Via Licio Giorgieri 1, 34127 Trieste, Italy*

Ovidio Catanzano, ...

*\*Institute for Polymers, Composites and Biomaterials (IPCB) – CNR, Via Campi Flegrei, 34, Pozzuoli,  
Naples, Italy.*

## Abstract

In this contribution we describe the preparation and characterization of a series of cross-linked films based on the combination of an elastin-derived biomimetic polypeptide (Human Elastin-Like Polypeptide, HELP) with alginate (ALG) to obtain a composite with enhanced properties. ALG/HELP composite films loaded with the hydrophobic natural antioxidant curcumin were prepared by solvent casting method followed by the cross-linking with calcium chloride. The compatibility between the two components as well as the final properties was evaluated. The micro-morphological study of films showed a homogeneous structure, but the film tensile strength decrease with HELP content and elongation at break was adversely affected by biopolymer addition. Spectroscopic and thermal analyses confirmed an interaction between ALG and HELP which also causes a modification in swelling kinetics and faster degradation. Moreover, the study of curcumin release showed a controlled delivery up to 10 days with a faster release rate in the presence of HELP. Human Dermal Fibroblasts (hDF) were used to test the in vitro cytocompatibility. The antioxidant activity correlated to the increase of HELP content suggested the applicability of these

34 composites to develop smart biomaterials. Overall, these features indicated how this  
35 composite material has considerable potential as customizable platforms for various  
36 biomedical applications.

37

## 38 **Keywords**

39 Alginate

40 Human Elastin-Like Polypeptide

41 Structural and thermal characterization

42 Composite film

43 Drug delivery

44 Biomimetic material

45

## 46 **1. Introduction**

47 Natural polymers derived from microbial, plant, or animal sources have been extensively  
48 investigated for applications in regenerative medicine as they possess some structural  
49 similarities with the natural supporting structures of the body, such as connective tissues  
50 and extracellular matrix (ECM). They are non-toxic, biocompatible and particularly versatile  
51 and adaptable to technological needs, due to the presence of different functional groups in  
52 their structure. A large number of studies have been carried out to investigate the potential  
53 applications of natural polymers in regenerative medicine, exploring the relationship  
54 between the polymer nature, its physical form (such as hydrogels, microspheres,  
55 microcapsules, sponges, foams, and fibers) [1,2]. An efficient way to tune the biopolymer-  
56 based biomaterial properties, towards a wide range of biomedical applications, is their  
57 combination with other components (organic or inorganic) to prepare a new range of  
58 composites with unique properties. This approach allows the development of materials with  
59 specific features in terms of biodegradability, mechanical strength, gelation property and cell  
60 compatibility, possessing properties that are different from those of the original components.  
61 Moreover, composite materials allow a flexible design, since their structure and properties  
62 can be optimized and tailored to specific applications [3]. Alginate (ALG) represents a whole  
63 family of linear copolymers composed of both (1,4)-linked  $\beta$ -D-mannuronate (M) and  $\alpha$ -L-  
64 guluronate (G) residues in different proportions, mainly depending on the source. Physical  
65 properties and molecular weight of ALG strictly depend on the sequence of M and G units,  
66 as well as the cross-linking which occurs by the co-operative binding of divalent cations and

67 the G-block regions of the copolymer. To take advantage of the biocompatibility and  
68 biodegradability under physiological conditions, ALG is often used in combination with other  
69 materials, such as synthetic and natural polymers (Poly Lactic-co-Glycolic Acid (PLGA),  
70 Polyethylene Glycol (PEG), and chitosan), proteins (collagen and gelatin), ceramic  
71 materials, and bioactive glass to prepare new supports for tissue engineering [4–7]. Each of  
72 the reported composite material has its peculiar properties, however, the combination  
73 between ALG and proteins represents a promising strategy to enhance the cellular  
74 interaction of alginate and to tailor the biodegradability of the final materials for tissue  
75 regeneration [8]. Elastin is one of the most abundant proteins in the native ECM [9]. The  
76 high content of hydrophobic amino acids makes elastin one of the most chemically resistant  
77 and durable proteins in the entire body [9]. In nature, elastin has a fundamental role in the  
78 extracellular matrix as it confers rubber-like elasticity to the tissues, allowing them to sustain  
79 indefinite cycles of deformation/relaxation without rupture [10]. For this reason, elastin  
80 represents an attractive component for composite fabrication as it may provide elastic recoil  
81 to stiffer materials. Moreover, elastin interacts with cells via a large number of cell surface  
82 receptors, enhancing skin fibroblast, vascular smooth muscle cells and endothelial cells  
83 proliferation [11,12] and having a biological effect on acceleration and enhancement of skin  
84 wound repair [13]. Unfortunately, the hydrophobic nature of elastin and its extensive cross-  
85 linked structure makes it difficult to be processed into biomaterials [14]. Hence, soluble and  
86 recombinant forms of elastin such as tropoelastin, alpha-elastin, and synthetic elastin-like  
87 polypeptides (ELPs) have been used to prepare composite scaffolds [15]. Human Elastin-  
88 Like Polypeptides (HELPS) are a class of bio-inspired polypeptides developed as an  
89 alternative to the elastin of animal origin. HELPS are artificial, genetically encodable  
90 biopolymers based on the hexapeptidic VAPGVG repeated motif [16] that have proven to be  
91 excellent components for drug delivery and tissue engineering applications due to their good  
92 cyto- and bio-compatibility, their ease of handling, design, production, and modification [17].  
93 Furthermore, thanks to the presence of glutamine and lysine residues in their primary  
94 structure, HELPS can be cross-linked under the action of transglutaminase (TG) to form  
95 stable hydrogels without the use of harsh chemicals like glutaraldehyde or analogous cross-  
96 linking agents [18]. In previous works, we have synthesized and tested a series of HELPS  
97 with different structures and properties as adhesion substrates for muscle cells [19,20],  
98 model systems for elastolytic activity detection [21], and drug delivery devices [17,22].  
99 However, the potential of HELPS as a component of composite biomaterials has not been  
100 fully explored yet. Recently, a composite material based on the deposition of HELPS on

101 electrospun poly-L-lactic acid fibers (PLLA-HELP) was developed by our group  
102 demonstrating the suitability of this protein to prepare readily customizable biomaterials with  
103 specific functionality [23]. Here, we decided to assess the combination of HELP with a  
104 natural polymer (ALG) to obtain a composite with enhanced chemical-physical properties.  
105 Therefore, the aim of this work was to investigate the interactions between the two  
106 components and to evaluate the potential of the obtained composite to realize customizable  
107 platforms for drug delivery of multifunctional agents. A series of ALG-based polymeric films  
108 with different concentration of HELP were prepared and loaded with the model compound  
109 curcumin. As far as we know, this is the first study reporting the preparation of a biomaterial  
110 based on ALG and HELP for the delivery of a natural product.

111

## 112 **2. Experimental**

### 113 **2.1. Materials**

114 Sodiumalginate (Ph.Eur. grade, MW180–300 kDa, Lot. 9C260/DOC) was purchased from  
115 Carlo Erba reagents (Milano, Italy). Yeast extract, tryptone, NaCl and antibiotics for E. coli  
116 growth were from Duchefa Biochemie. For cell culture, Dulbecco's modified eagle medium  
117 (DMEM) was purchased from Lonza Group (Basel, Switzerland), fetal bovine serum (FBS),  
118 penicillin/streptomycin solution and trypsin/ EDTA solution were from Aurogene (Rome,  
119 Italy), and Resazurin sodium salt was from Alfa Aesar (Ward Hill, MA, USA). Curcumin, 2,  
120 2- diphenil-1-picrylhydrazyl (DPPH) and all the other products and chemicals used during  
121 the experiments were obtained from Sigma Aldrich (St. Louis, USA) and were of reagent  
122 grade with the highest purity available. Deionized ultra-filtered water was used throughout  
123 this study.

124

### 125 **2.2. Production of HELP polypeptide**

126 HELP recombinant biopolymer was prepared as previously reported [21]. The recombinant  
127 product was expressed in a C3037 E. coli strain (New England Biolabs, Ipswich, MA) and  
128 then subjected to an extraction and purification procedure exploiting its inverse phase  
129 transition properties. Briefly, the pellet obtained from 1.2 l of IPTG-induced bacterial culture  
130 was re-suspended in 400 ml of extraction buffer (50 mM Tris/ HCl pH = 8, 250 mM NaCl,  
131 0,1 mM EDTA, 0,1% Triton X-100, 1 mM PMSF) and disrupted using a high-pressure  
132 homogenizer (Panda NS1001L, GEA Niro Soavi, Germany). To eliminate the solid bacterial  
133 residues, the recovered suspension was added with 20 mM 2- mercaptoethanol, cooled on

134 ice, and finally centrifuged at 10000 rpm, for 30min at 8 °C (Beckman–Coulter, J-26 XP).  
135 The separation of the recombinant biopolymers of interest from the supernatant was  
136 obtained using a series of temperature-dependent transition cycles. Aggregated HELP  
137 polypeptide particles were obtained adding NaCl to a final concentration of 0.5 M at 37 °C  
138 and separated by centrifugation at 10000 rpm, 37 °C for 30 min. The pellet was re-dissolved  
139 in cold water and all the non-soluble material was discarded by cold centrifugation (10,000  
140 rpm, 8 °C for 10 min). The temperature of the resulting solution was raised to 37 °C and the  
141 protein was precipitated again by NaCl addition. Three of these cycles were sufficient to  
142 obtain the pure recombinant protein. The polypeptide was frozen overnight at –80 °C, and  
143 then lyophilized at 0.01 atm and –60 °C in a Modulyo apparatus (Edwards, Crawley, UK) for  
144 long-term storage. The HELP recombinant polypeptide obtained was analyzed by sodium  
145 dodecyl sulfate – polyacrylamide gel electrophoresis (SDS-PAGE).

### 147 **2.3. Preparation of alginate/HELP composite film**

148 The ALG/HELP composite films were prepared by solvent casting method. The entire  
149 preparation procedure is summarized in Fig. 1. Alginate (1% w/v) was dissolved in ultrapure  
150 water together with HELP at two different concentrations (0.125 and 0.25% w/v) and glycerol  
151 (2:1 w/w alginate/glycerol). The mixture was kept under magnetic stirring at 4 °C, for at least  
152 6 h. A solution of curcumin in acetone (20 mg/ml) was added to the resultant ALG/HELP gel  
153 to obtain a final concentration of 0,1% w/v. The curcumin-loaded ALG/HELP gel was gently  
154 mixed under magnetic stirring, at 4 °C for 30 min. 4 ml of this dispersion was then poured  
155 into Petri dishes with a diameter of 35 mm and left overnight in an oven at 37 °C, to favor  
156 solvent evaporation. Three different films, named ALCur 1 (no HELP) HALCur 1 (0.125%  
157 w/v HELP) and HALCur 2 (0.25% w/v HELP) all loaded with the same amount of curcumin  
158 were prepared to test the effect of the presence of HELP on the properties of the composites.  
159 Moreover, an ALG alone film without curcumin (Ca-ALG) was prepared as described above  
160 as control for FTIR and thermal analysis. All the dried films were crosslinked by immersion  
161 in a solution of calcium chloride 5% (w/v) for 15 min. After crosslinking, the samples were  
162 washed with abundant ultrapure water several times and further dried in the oven to obtain  
163 the final films. After preparation, all the films were visually examined to identify any physical  
164 defects.

### 166 **2.4. Scanning electron microscopy (SEM)**

167 The morphology of film surfaces was evaluated, by using a scanning electron microscope  
168 (Philips 501, Holland). Films were freeze-dried for 24 h with an Alpha 2–4 LCS Plus freeze  
169 dryer (Martin Christ, Osterode am Harz, Germany) and the anhydrous hydrogels were then  
170 coated with gold (thickness 60 nm).

171

## 172 **2.5. Mechanical characterization**

173 Mechanical properties of ALCur, HALCur 1 and HALCur 2 were evaluated by using a traction  
174 dynamometer (Acquati AG MC1, Italy). Before the traction test, the films were accurately cut  
175 in rectangles with a predetermined size of 25 Å~ 16mm. Each sample was tested in triplicate.  
176 The traction tests were performed by setting the following parameters: pre-fixed distance  
177 between clips, ±14.5 mm; traction speed, 25 mm/ min<sup>-1</sup> (longitudinal), 5 daN top head.  
178 Applied Force and movement (sample stretching and elongation) were recorded and  
179 digitalized by PowerLab® 4/35 and by LabChart® Pro software, respectively. Strength and  
180 elongation were continuously registered till sample breakage. Before the traction tests, width  
181 and length of specimens were measured by a caliper while their thicknesses were measured  
182 by a digital micrometer (Mitutoyo Corporation, Japan). These values were used to obtain  
183 the cross-section area, a necessary value required for the calculation of applied stress after  
184 dynamometric measurements (stress  $\sigma$  = applied Force/cross section Area). Finally,  
185 stress/strain curves were drawn; only linear portion of tendencies (elastic behavior portion)  
186 was taken into consideration and their slope, corresponding to the elastic modulus,  
187 calculated.

188

## 189 **2.6. Attenuated total reflectance Fourier transform infra-red (ATR FT- 190 IR) analysis**

191 FTIR spectra were obtained in the attenuated total reflection mode (ATR), using a Perkin-  
192 Elmer spectrometer (Norwalk, CT, USA) equipped with universal-ATR accessory, fitted with  
193 a diamond optical element and ZnSe focusing elements. The apparatus operates with a  
194 single reflection at an incident angle of 45°. The analysis was carried out on Films at room  
195 temperature and ambient humidity. For each spectrum, 32 scans were acquired between  
196 4000 and 650 cm<sup>-1</sup> with a spectral resolution of 2 cm<sup>-1</sup>.

197

## 198 **2.7. Differential scanning calorimetry (DSC) and Thermogravimetric 199 analysis (TGA)**

200 Thermal properties of films were investigated by using a TA DSCQ2000 differential scanning  
201 calorimeter, equipped with a TA Instruments DSC cooling system. Dry nitrogen gas with a  
202 flow rate of 20 ml/min was purged thorough the cell during the measurements and the  
203 thermal treatments. Samples of approximatively 5 mg were heated from 20 to 200 °C and  
204 kept at this temperature for 2 min, then cooled from 200 to 25 °C, kept at this temperature  
205 for 2 min and re-heated from 25 to 200 °C. Heating/cooling rate was fixed to 20 °C/min in all  
206 the experiments. To determine the glass transition temperature of alginate the following  
207 thermal procedure was applied: samples were heated from 20 to 130 °C at 20 °C/min, kept  
208 at this temperature for 1 h, cooled to 20 °C, and re-heated to 200 °C at 20 °C/min. The  
209 thermogravimetric analysis (TGA) analysis has been widely used to study the thermal  
210 stability and thermal decomposition of polymers with increasing temperature. The TGA was  
211 carried out using a Perkin-Elmer Pyris Diamond TG-DTA apparatus in a nitrogen  
212 atmosphere to prevent thermal oxidation. Samples of about 5 mg were heated from 20 to  
213 600 °C at 10 °C/min with a nominal gas flow of 30 ml/min.

214

## 215 **2.8. Swelling study**

216 The swelling degree was monitored by measuring water uptake as a function of time. The  
217 initial weight of each sample was accurately recorded using an analytical scale, and then  
218 they were placed in 5 ml of water in a thermostatic bath at 37 °C. Samples were taken out,  
219 excess water was carefully removed using tissue paper, and after being weighed were re-  
220 immersed in water. The sample weight was recorded at intervals of 15min up to 1 h and  
221 then after 2, 4, 6 and 24 h (until equilibrium was established). Water was replaced after  
222 every weight measurement. The percentage swelling ratio (SR%) at each time point was  
223 calculated using Eq. (1):

224

$$225 \quad SR\% = \frac{W - W_0}{W_0} \times 100 \quad (1)$$

226

227

228 Where  $W$  is the mass of the swollen sample and  $W_0$  is the mass of the initial dry sample.  
229 Assuming that the network swells uniformly in all directions, the equilibrium water content  
(EWC) can be defined as the ratio between the weight of the swollen sample after 24 h in



230 water and its initial weight. The equilibrium water content (EWC) percent was calculated by  
231 Eq. (2):

232

$$\text{EWC (\%)} = \frac{W_e - W_d}{W_e} \times 100 \quad (2)$$

233

234

235 where  $W_e$  is the mass of the swollen sample at equilibrium and  $W_d$  is the mass of the dry  
236 sample at equilibrium.

237

## 238 **2.9. Film stability**

239 The stability of ALCur, HALCur 1 and HALCur 2 films was evaluated by placing them in  
240 phosphate buffer saline (PBS, NaCl 120 mM, KCl 2.7 mM,  $\text{Na}_2\text{HPO}_4$  10 mM) at pH 7.4, and  
241 monitoring weight change with time. Weighed samples were soaked in PBS at 37 °C up to  
242 14 days. At predetermined time intervals (0.5, 1, 6 and 14 days), films (n = 4) were removed  
243 from phosphate buffer, gently washed with ultrapure water to eliminate any soluble residue,  
244 and dried overnight in an oven at 37 °C. The weight loss (%) was calculated as the difference  
245 between the initial dry weight of the films (W) and the dry weight after incubation ( $W_0$ )  
246 according to the Eq. (3).

247

$$\text{Weight loss (\%)} = \frac{W - W_0}{W_0} \times 100 \quad (3)$$

248

249

## 250 **2.10. Study of curcumin release**

251 The study of curcumin release from ALCur, HALCur 1 and HALCur 2 films was carried out  
252 by soaking the films in 10ml of PBS (pH 7.4) modified with Tween 80 (10% v/v). Tween 80  
253 increases the solubility of curcumin in PBS, preventing the saturation of the release media,  
254 and reasonably simulates the in vivo conditions in which films could be applied. The  
255 Samples were kept under constant stirring at 40 rpm in a water bath shaker at 37 °C. During  
256 the release test period (0–10 days), at scheduled times, 1 ml of release medium was  
257 withdrawn, and replaced with the same volume of fresh medium. The concentration of  
258 released curcumin was determined using a UV–vis spectrophotometer (Synergy H1,

259 BioTek, Winooski, VT), by measuring the absorbance at 426 nm of collected samples.  
260 Experiments were performed in triplicate ( $n = 3$ ) and the mean cumulative percentage drug  
261 release was calculated using a standard calibration curve. The linearity of the response was  
262 verified over the concentration range 0,22–22  $\mu\text{g/ml}$  ( $r_2=0.999$ ).

263

## 264 **2.11. Biological investigation**

### 265 2.11.1. In vitro cell culture

266 Biological investigations on curcumin loaded composite films were performed using human  
267 dermal fibroblasts (hDF). hDF coded as C84 were isolated and expanded, starting from an  
268 underarm explant from a healthy, normolipaemic 45-years old female, and used at passage  
269 28. hDF were cultured in 75  $\text{cm}^2$  cell culture flask in Dulbecco's Modified Eagle Medium  
270 (DMEM) supplemented with 10% Fetal Bovine Serum (FBS), antibiotic solution  
271 (streptomycin 100  $\mu\text{g/ml}$  and penicillin 100 U/ml, Sigma Chem. Co) and 2 mM L-glutamine.  
272 hDF were incubated at 37 °C in a wet atmosphere with 5%  $\text{CO}_2$  and 95% air.

273

### 274 2.11.2. Cytotoxicity assay

275 Biocompatibility represents the first requirement for a medication intended for direct  
276 application on injured skin. Toxicity assays of the three types of films developed were  
277 assessed in triplicate by first culturing hDF on them, and then evaluating cell viability over  
278 48 h using resazurin assay. ALCur, HALCur 1 and HALCur 2 films were cut in 5 mm disk  
279 and sterilized by immersion in a stock penicillin/streptomycin antibiotic solution ( $1 \text{ } \mu\text{g/ml} \sim 10^7 \text{ U/l}$ )  
280 for 1 h, followed by 2 washes in sterile ultrapure water and subsequently kept under the  
281 safety cabinet till drying. Once dehydrated, scaffolds were placed in a 96 well-plate and  
282 seeded with hDF. Cells were harvested from the culture flasks at the confluent state by  
283 incubation with trypsin solution for 2 min at 37 °C. Cells were then re-suspended with 10%  
284 serum-supplemented DMEM, counted and plated at density of  $3 \times 10^4$  cells/well onto the  
285 scaffolds. 100  $\mu\text{l}$  of cells resuspension was placed on each scaffold. The same number of  
286 cells incubated in the same condition in absence of films was considered as untreated  
287 control. Cell viability was evaluated on the basis of the ability to convert resazurin into its  
288 fluorescent derivative resarufin. Briefly, at each time point (24; 48 h), scaffolds were  
289 transferred into a clear dark 48-well plate and washed with PBS. 300  $\mu\text{l}$  of resazurin solution  
290 (250  $\mu\text{g/ml}$ ) in DMEM without phenol red with 10% FBS were then added to each well and  
291 incubated overnight at 37 °C in the dark. Fluorescence was recorded at 560 nm excitation

292 and 590 nm emission by a Spark® microplate reader (Tecan, Switzerland). Absorbance  
293 obtained from correspondent empty scaffolds was subtracted from each measurement.

294

## 295 **2.12. Antioxidant activity**

296 Antioxidant scavenging activity of the curcumin loaded films was measured by DPPH test.  
297 This colorimetric assay consists of the occurring of the scavenging chemical reaction  
298 between a solution of the stable radical 2, 2-diphenyl-1-picrylhydrazyl (DPPH) with the  
299 supposed antioxidant compound. The reaction changes the DPPH UV absorption band  
300 decreasing its optical absorption at 517 nm when the DPPH molecule is reduced from an  
301 antioxidant compound (turning color of the solution from violet to yellow). Briefly, a test  
302 solution composed of 8.5 ml of acetonitrile, 1 ml of a stock solution of DPPH 1 mM in ethanol  
303 (final concentration 100 μM), and 0.5 ml of deionized water was prepared before the  
304 experiment. The test specimens (disks with diameter 1.5 cm) were placed in an amber jar  
305 (n = 3) together with 10 ml of the test solution and kept under stirring in the dark on an orbital  
306 shaker for 60 min at room temperature. A control sample consisting of an amber jar  
307 containing 10 ml of test solution was also measured as a control sample. At predetermined  
308 time intervals (each 20min), 1 ml of the sample was collected and the vials were immediately  
309 replenished with an equivalent volume of test solution. The absorbance of the collected  
310 samples was systematically read through a Perkin Elmer - Lambda 25 spectrophotometer  
311 measuring the absorbance at 517 nm. A solution of ethanol/deionized Water (95:5 v/v) was  
312 used as blank sample during the measurement. The scavenging percentage at each time  
313 point was calculated as Eq. (4).

314

$$315 \quad SR\% = \frac{W - W_0}{W_0} \times 100 \quad (1)$$

316

317

318 where  $A_0$  is the absorbance of the control sample and  $A$  is the absorbance in the presence  
319 of the sample at any time. Decoloration and subsequent decrease of absorbance at 517 nm  
320 indicated proportional antioxidant charge increase of the sample tested.

321

## 321 **2.13. Statistical analysis**

322 Statistical analyses were undertaken using GraphPad Prism®, version 6.00 (GraphPad  
323 Software, La Jolla California USA) using one-way ANOVA test. All experiments were  
324 performed in triplicate and the results were expressed as the mean ± standard deviation  
325 (SD). A p-values below 0.05 considered as significant. 3. Results and discussion

326

327

## 328 **3. Results and discussion**

### 329 **3.1. Preparation of composite films**

330

331 Native body tissues can be viewed as complex materials since they include several  
332 extracellularmatrix components with different features and properties. For this reason, a  
333 one-component material cannot be used to fully replicate the complex mechanics and the  
334 biochemical attributes of tissues. Despite the extensive description of elastin and elastin like  
335 peptides use to prepare cross-linked gels, fibers, or injectable scaffolds for tissue  
336 engineering and drug delivery [3,13,15,24] their use in applications such as wound dressing  
337 or regenerative medicine has to be further improved. The preparation of a composite  
338 material based on the natural polymer alginate loaded with a recombinant form of the Human  
339 Elastin-Like Polypeptide (HELP) well described and characterized by our group [25,26]  
340 represents a valuable approach to reach this goal. In our laboratory, synthetic genes based  
341 on the repeated hexapeptidic motifs that characterize human tropoelastin have been cloned  
342 and the expression products were purified through inverse transition cycling [26]. The  
343 recombinant technology used to produce HELPs provides precise control over the structure  
344 and properties of the final polypeptide resulting in highly homogeneous derived materials.  
345 Moreover, the purification of expressed HELP achieved through the inverse phase  
346 transition, allows obtaining a highly purified recombinant polypeptide. Composite films with  
347 (HALCur 1 and HALCur 2) and without (ALCur) HELP were prepared by solvent casting  
348 followed by the crosslinking, using a calcium chloride solution (Fig. S1). The physical  
349 interactions between alginate chains and calcium ions leads to the formation of a well-  
350 defined structure, popularly known as the “egg-box model”, in which  $Ca_{2+}$  ions are embodied  
351 in cavities like eggs in a cardboard egg box [27,28]. The resulting chain-to-chain interactions  
352 that are formed with the crosslinking increase the structural cohesion of the alginate-based  
353 films, leading to higher values of tensile strength and low solubility in water [29]. The same  
354 curcumin loading was employed to assess the effect of HELP on the final composite film  
355 properties. Glycerol was added as a plasticizer to all the formulations to increase the

356 handling properties and to facilitate the removal from the Petri dish [30]. After crosslinking,  
357 the films were flexible, transparent, and uniform with no evident physical defects. The  
358 addition of curcumin conferred a yellowish color to these composite films compared to Ca-  
359 ALG films that were transparent. A more accurate examination of the surfaces of the  
360 composite films was carried out by SEM imaging. Representative SEM micrographs at the  
361 same magnification of the tested specimens are compared in Fig. 2. All films displayed a  
362 homogeneous structure without any large cracks, air bubbles or evident sign of phase  
363 separations, which indicate a good quality polymeric film. However, in presence of HELP  
364 the images shown a heterogeneous surface with small aggregates that seems to be  
365 influenced by concentration. In particular, ALCur presents a quite smooth surface,  
366 characterized by few imperfections consisting of soft protuberances at the surface. These  
367 structures increase in terms of numbers proportionally with HELP's increase, becoming  
368 almost fibrillar elements ( $\pm 10 \mu\text{m}$  in length) in the most concentrated sample (Fig. 2C).  
369 Different roughness could have an influence on cell behavior in contact with the films tested,  
370 however, the biological investigation did not show significant pieces of evidence of  
371 enhancement rather than inhibition of cell viability.

372

## 373 **3.2. Film characterization**

### 374 3.2.1. Mechanical properties

375 The mechanical properties of biomaterials, in particular those designed for tissue  
376 applications, need to be carefully characterized to fulfil the requisites for a targeted  
377 application. The ability to resist to mechanical stress of a material is a valuable physical  
378 property that can affect the material behavior both for the manipulation and for the  
379 adaptation to the tissues. With the dispersion of HELP into the alginate matrix, we aimed to  
380 increase the flexibility of the composite material to make it suitable in applications as skin  
381 substitutes and wound dressings, where a degree of elasticity is essential [31,32]. The  
382 elastic deformation of a material is well represented by Young's modulus and by the percent  
383 elongation at break ( $\epsilon_{\text{break}}$ ), both reported in Table 1. While the values found for ALCur are in  
384 agreement with what reported in literature for a calcium-crosslinked alginate [33], the  
385 addition of HELP significantly increases Young's modulus and reduces the  $\epsilon_{\text{break}}$ , resulting in  
386 an increase in the hardness with increasing concentration of HELP (Fig. S3). This effect can  
387 be attributed to the formation of a closer network in presence of HELP, due to molecular  
388 entanglements, as will be described in detail in the next paragraphs. The worsening of the  
389 mechanical properties of the composites with increasing concentration of HELP can be

390 attributed to alignment, compatibility and specific interactions of the polypeptide with the  
391 alginate chains. Further work is in progress to better investigate this point. However, the  
392 maximum applied force (the force applied to the sample at the moment of breaking) doesn't  
393 present any significant difference among the specimen tested and can be considered high  
394 enough to allow easy manipulation of the films avoiding breakage.

395

### 396 3.2.2. FT-IR

397 Spectra of HALCur 2 and HELP are compared with a crosslinked ALG film without curcumin  
398 (Ca-ALG) in Fig. 3a (spectrum of HALCur 1 is not reported since peaks of HELP were hardly  
399 detectable). HELP shows diagnostic bands at  $\sim 3495$  ( $\text{N-H}$  stretching), 3288 ( $\text{N-H}$   
400 stretching), 3053 and 2964 ( $\text{C-H}$  stretching), 1636 (amide I,  $\text{C=O}$  stretching), 1533 (amide  
401 II,  $\text{N-H}$  bending). In HALCur 2, the amide I band is hidden by the strong band of curcumin  
402 at  $1620\text{ cm}^{-1}$ , whereas a shift of amide II band to a lower frequency ( $1514\text{ cm}^{-1}$ ) is detected.  
403 This shift accounts for the establishment of interactions between the  $\text{N-H}$  amidic groups of  
404 HELP and ALG via hydrogen bonds, as described in details below. No appearance of new  
405 bands was detected, indicating that no chemical reaction occurs. From the analysis of the  
406 FT-IR spectra obtained from sodium alginate (Na-ALG) and the corresponding crosslinked  
407 film (Ca-ALG) (Supplementary material S2), we found that when crosslinked with calcium  
408 ions, the ALG bands of carboxylate respectively moved from  $1593$  to  $1587\text{ cm}^{-1}$  and from  
409  $1403$  to  $1413\text{ cm}^{-1}$  (Fig. S2). This shift at higher frequency of the symmetric band is a well  
410 known indication of  $\text{Na}^+/\text{Ca}^{2+}$  exchange [34]. In the spectrum of HALCur 2 specimen both the  
411 asymmetric and symmetric  $\text{C=O}$  stretching peaks of ALG carboxylate shift towards higher  
412 frequencies ( $1594$  and  $1427\text{ cm}^{-1}$  respectively) compared to Ca-ALG. This suggests the  
413 establishment of interactions between HELP and carboxylate, that might have an impact on  
414 coordination bond between  $\text{Ca}^{2+}$  and ALG, affecting crosslinking; in fact the frequency  
415 separation between  $\text{C=O}$  asymmetric and symmetric stretches ( $\Delta\nu_{\text{a-s}}$ ), decreases to  $164$   
416  $\text{cm}^{-1}$ , which is somewhat lower than in the case of Ca-ALG (Supplementary material S2).  
417  $\Delta\nu_{\text{a-s}}$  values well below  $200\text{ cm}^{-1}$  are compatible with the so-called bidentate "pseudo-  
418 bridging" coordination arrangement, in which one of the two oxygen atoms is hydrogen  
419 bonded to water or another ligand. Therefore, formation of hydrogen bonds between  
420 carboxylate and  $\text{N-H}$  of amidic groups of HELP can be envisaged, as proposed in Fig. 3b.  
421 According to literature [35], FTIR spectrum of pure curcumin have a series of major peaks  
422 at  $3508\text{ cm}^{-1}$  (free  $\text{O-H}$  stretching of phenol group),  $\sim 3300\text{ cm}^{-1}$  ( $\text{-OH}$  stretching),  $1620\text{ cm}^{-1}$   
423 (mixed  $\text{C=O}$  and  $\text{C=C}$  stretching),  $1601\text{ cm}^{-1}$  (aromatic  $\text{C=C}$  stretching),  $1505\text{ cm}^{-1}$  ( $\text{C=O}$

424 stretching) and 1270  $\text{cm}^{-1}$  (enol  $\text{C}=\text{O}$  stretching). Furthermore, the peaks at 713, 856, 886  
425 and 961  $\text{cm}^{-1}$  indicate the bending vibrations of  $\text{C}-\text{C}-\text{H}$  and  $\text{C}-\text{H}$  bond of aromatic ring (Fig.  
426 S3, Supplementary material). Peaks of curcumin and ALG are retained at the same  
427 frequency in ALCur (not shown), indicating the absence of interactions with ALG, whereas  
428 a shift of the  $\text{C}=\text{O}$  band of curcumin to 1282  $\text{cm}^{-1}$  was found in HALCur 2. This can be  
429 considered an evidence of complex formation, likely involving hydrophobic sequences of  
430 HELP.

431

### 432 3.2.3. Differential scanning calorimetry (DSC) and thermogravimetric analysis (TGA)

433 The thermal behavior of the curcumin-loaded films was analyzed by DSC. Raw ALG  
434 thermogram exhibited an exothermic peak at 242 °C, resulting from polymer degradation.  
435 In the thermogram of all crosslinked samples, this peak disappeared due to the formation of  
436 an “egg-box” structure around calcium ions, which increases the degradation temperature  
437 of ALG [36]. The thermogram of curcumin showed a very sharp endothermic peak at 182  
438 °C with an associated melting enthalpy of 137,6 J/g. In ALCur, the peak was still present,  
439 but shifted to a lower temperature and appeared broadened (168,9 °C, 130.8 J/g). The  
440 dispersion within the alginate matrix limits the capability of curcumin to crystallize, as  
441 demonstrated by the decrease of melting temperature. In the presence of HELP, the melting  
442 endotherm completely disappeared in both HALCur 1 and HALCur 2 thermograms. These  
443 results suggest the occurrence of interactions with HELP that prevent the crystallization of  
444 curcumin. The glass transition temperature ( $T_g$ ) of ALG in crosslinked samples was  
445 determined during the second run after complete removal of water.  $T_g$  of raw ALG was not  
446 reported because not reliably detectable. The complete results are reported in Table 2. The  
447 addition of HELP to film formulation causes an increase of alginate  $T_g$ , likely due to  
448 interactions of the polypeptide with carboxylate group, as previously described in the FT-IR  
449 analysis paragraph, thus confirming that presence of HELP can modify the crosslinking  
450 strength and density.  $T_g$  increases proportionally to the HELP content, as expected. To  
451 further explore the interaction between HELP and the crosslinked alginate matrix, the  
452 composite films were characterized by TGA from 20 to 600 °C, recording the weight loss as  
453 a function of temperatures. Thermogravimetric analysis was performed to study polymer  
454 degradation, which is influenced by physical interactions between the components and to  
455 evaluate the water content of different samples. Table 2 lists the weight loss up to 150 °C,  
456 the onset temperature ( $T_{\text{onset}}$ ) of the whole degradation process, and the temperature of the  
457 maximum degradation rate, which corresponds to peaks in the derivative plot ( $T_{\text{peak}}$ ). Fig. 4a

458 and b shows the weight loss curve and its derivative (DTG) as a function of temperature,  
459 respectively. The HELP thermogram shows a sharp degradation from 190 to 400 °C, with a  
460 maximum weight loss at 327 °C (12.28%/min), while degradation of curcumin occurs  
461 between 175 and 545 °C with a maximum weight loss at 362 °C (4.72%/min). The raw  
462 alginate and all the crosslinked samples (ALCur, HALCur 1 and HALCur 2), thermograms  
463 show two different weight loss events. The first weight loss (around 15%) up to 150 °C  
464 corresponds to the evaporation of water [37]. The second stage above 200 °C is related to  
465 degradation phenomena. The derivative thermogravimetry (DTG) curves show the thermal  
466 events in the region where degradation occurs (Fig. 4b). DTG curve of ALG shows a single  
467 peak with a maximum at around 246 °C (15.82% 7 min), related to thermal degradation of  
468 both mannuronic and guluronic units. In the case of Ca-ALG, two partially overlapping  
469 events can be distinguished, suggesting that two structures with different degradation  
470 profiles coexist. These different phenomena are related to mannurate and guluronate  
471 segments (peak1 and peak2, respectively) [38,39], which are differently involved into the  
472 polymer three-dimensional network. In particular, mannuronic moieties, which are not  
473 involved in crosslinking, undergo an early degradation ( $T_{\text{peak 1}}$  232 °C), whereas guluronic  
474 units degrade at a higher temperature ( $T_{\text{peak 2}}$  259 °C) since they tightly interact with calcium  
475 ions in the egg-box structure. In the thermograms of HALCur samples, a single-step  
476 degradation curve, mainly attributed to ALG, is detected. This evidence is consistent with  
477 physical interactions, via hydrogen bonds, between HELP and ALG chains. Moreover, the  
478 addition of HELP to film formulation results in an increase of guluronic moieties degradation  
479 temperature. This result suggests that HELP interacts preferentially with guluronic units, and  
480 is entangled in the three-dimensional polymer network. In the case of HALCur 2, degradation  
481 temperature of guluronate segments increases of around 20 °C with respect to Ca-ALG,  
482 thus demonstrating that a higher amount of HELP significantly stabilizes alginate crosslinks.  
483

#### 484 3.2.4. Swelling, equilibrium water content and stability

485 The ability of a material to absorb water depends on its physical structure and it is related  
486 to specific material properties as a uniform and prolonged release of the drug and  
487 bioadhesion potential [40]. Swelling of HAL films in PBS was investigated in water and the  
488 differences in swelling capacity depending on the amount of HELP content are shown in Fig.  
489 5A. The water uptake of the composite films was rapid and reached its maximum 1 h after  
490 contact with water. The curves show that after 1 h the maximum swelling was achieved for  
491 all the formulations (81.0% ± 4.2, 90.0% ± 3.8, 90.4% ± 3.5 for ALCur, HALCur 1, HALCur



492 2 respectively) with a significantly ( $p < 0.05$ ) higher percentage swelling for the HALCur 1  
493 and HALCur 2 films. No significant differences in the swelling ratio were found between  
494 HALCur 1 and HALCur 2 throughout the experiment. The swelling behavior was followed for  
495 24 h and a slight swelling decrease percentage, probably due to a material loss, was  
496 observed. However, after 24 h significant differences are still found in swelling between the  
497 samples. HELP affects also the total amount of water that these systems can absorb. The  
498 EWC of HALCur 1 and HALCur 2 are  $43.6\% \pm 0.8$  and  $45.5\% \pm 1.8$  respectively, significantly  
499 higher if compared with the  $40.9\% \pm 2.2$  recorded for the ALCur film. The stability profiles of  
500 the HAL films in physiological conditions were investigated, monitoring weight changes with  
501 time. At each time point, HALCur 1 and HALCur 2 films showed higher degradation than the  
502 ALCur. After 7 days of incubation, the films containing HELP appeared more fragile and at  
503 12–14 days of incubation no insoluble material could be detected after visual inspection (Fig.  
504 5B). In our hypothesis, this degradation behavior may further confirm the interactions  
505 between the HELP and the carboxylate group of alginate previously detected by FT-IR,  
506 DSC, and TGA. In HALCur 1 and HALCur 2 a weight loss of about 30% is already evident  
507 after 12 h and it could be attributed to the easy solubilization in the aqueous release media  
508 of the HELP fraction, with the consequent weakening of the entire film structure.

509

### 510 **3.3. Curcumin release**

511 The release profile of curcumin from HAL composite films was assessed in PBS at pH 7.4  
512 and  $37\text{ }^{\circ}\text{C}$ , simulating physiological conditions. Curcumin in the loaded films showed  
513 controlled release profiles with a limited initial burst (Fig. 6). After 10 days, over 60% of the  
514 total curcumin contained in the films was released with significant differences in the release  
515 rate depending on the formulation tested. These differences are more evident during the  
516 first 8 h, where the release rate steadily increases to reach a total percent release of  $15.46$   
517  $\pm 2.45$ ,  $21.28 \pm 1.93$ ,  $29.40 \pm 3.23$  for ALCur, HALCur 1, and HALCur 2 respectively (Fig. 6,  
518 inset). The release experiments were conducted up to 10 days to carefully assess both short  
519 and long-term release dynamics, as well as the capability of the films to retain the curcumin.  
520 Even for a longer period, the amount of curcumin released into the soaking medium is higher  
521 in the presence of HELP, with a rising trend correlated to the total HELP amounts. The drug  
522 release from the swellable scaffolds mainly depends on water uptake kinetics, pointing to  
523 the presence of HELP as a key parameter in affecting the release rate. As previously  
524 discussed, films containing HELP have higher water uptake, a feature that appears to be  
525 related to the release profile as well. The presence of HELP into an alginate matrix o film

526 can therefore also be used to control the release of a hydrophobic drug, modifying the  
527 structural features of the matrix and tuning the release of the loaded drug.

528

### 529 **3.4. Cytotoxicity assay**

530 Biological studies were conducted to demonstrate if the developed composites, differing  
531 each other for HELP content (0 to 0.25%), did not show toxic effects on human dermal cells.  
532 The second aim of this study consisted in the evaluation of cell proliferation induction due  
533 to the presence of HELP in the composites. The in vitro cytotoxicity evaluation is a fast  
534 method to provide predictive evidence of material biocompatibility. Cytotoxicity of  
535 ALG/HELP composites was evaluated on human dermal fibroblasts (hDF), which play an  
536 important role in generating connective tissue and allowing the skin to recover from injury  
537 [41]. Fig. 7 shows the effect of the films on the viability of hDF assessed by resazurin assay.  
538 After 24 h of incubation, the ALCur replicas showed the lowest cell viability ( $63\% \pm 9$ ),  
539 comparing it with the control group. HALCur 1 and HALCur 2 showed a viability of  $80\% \pm 1$   
540 and  $72\% \pm 4$ , respectively. The evaluation at 48 h, ALCur had the lower viability of  $60\% \pm 4$ ,  
541 HALCur 1 scored  $73\% \pm 8$  and HALCur 2,  $72\% \pm 5$ . At both these time points, the cell viability  
542 of ALCur is still around 60% while for HALCur 1 and HALCur 2 viability is significantly higher.  
543 According to the recommended guidelines for the evaluation of in vitro cytotoxicity for  
544 medical devices and delivery systems (DIN EN ISO 10993-5), a biomaterial can be deemed  
545 non-cytotoxic if the cell viability after exposure does not fall below the 70% [42]. The ALCur  
546 films resulted in the lowest values in terms of viability respect the controls, Conversely, in  
547 the presence of HELP in all cases the cell viability is higher of 70% both at 24 and 48 h.  
548 These data suggest a cell proliferation enhancement effect of HELP on hDF, and this is  
549 consistent with the previous observation that elastin like polypeptides may exert a pro-  
550 proliferative effect [43]. Therefore, the results obtained in the present study show that the  
551 HAL composite films loaded with curcumin could be considered as potentially biocompatible  
552 and generally safe.

### 552 3.5. Antioxidant activity

553 It is well known that chronic skin wound oxidation represents a major etiological cause of macromolecular damages during the tissue  
554 regeneration process. ECM proteins, in particular, can be damaged by Reactive Oxygen  
555 Species (ROS) activity due to their high chemical reactivity and capability to oxidize cellular  
556 macromolecules [44]. ROS are produced in significant amounts from macrophages invading  
557 the wound area during inflammation, playing a crucial role as signalling molecules as well  
558 as antimicrobial compounds [45]. However, the prolonged tissue exposition to high  
559 concentrations of oxidative stress gives a significant contribution both to the insurgence and

560 persistence of chronic wounds and other pathologies. The natural phenolic compound  
561 Curcumin has well demonstrated antioxidant and anti-inflammatory effects by carrying out  
562 scavenging activity of free radicals, lowering lipid peroxides [46–48]. These inherent  
563 properties make curcumin particularly suitable for the treatment of various damaged tissues,  
564 as wound injuries. In particular, its antioxidant and radical scavenging activity can be  
565 exploited to control wound oxidative stress and thereby accelerate wound healing [46,49].  
566 Animal studies suggest that supplementation of this compound could enhance/ ameliorate  
567 the tissue repair process [50]. In this work, we performed an antioxidant scavenging activity  
568 assay to verify if the antioxidant activity of curcumin is maintained even after dispersion in  
569 ALG/HELP films. The results (Fig. 8), confirmed the strong in vitro antioxidant activity of the  
570 developed alginate-based composites containing curcumin 0.1% w/w. As expected, no  
571 significant differences were detected among the sampling time points. In particular, in all the  
572 samples tested the scavenging activity on DPPH molecule ranged from  $66.2 \pm 4.7\%$  to  $84.9$   
573  $\pm 4.5\%$ . Interestingly, the difference in the antioxidant activity observed among the samples  
574 that were analyzed at later time points appeared related to the presence of HELP in the  
575 composite. This suggests that the HELP component favours the release of the curcumin  
576 although further studies are needed to support these results. In conclusion, the composites  
577 resulted effective as free radical scavengers showing the potential application in medical  
578 devices that can improve the wound healing process and proper skin regeneration.

579

580

581

## 582 **4. Conclusion**

583 This study aimed to test the properties of a series of composite films based on the natural  
584 polymer alginate and a recombinant form of human elastin that can be loaded with bioactive  
585 components. There are only a few examples of elastin-like based composites that have  
586 been developed till now, and with this work, we have demonstrated how the combination of  
587 alginate and HELP allowed tuning the final properties of the resulting material, thus  
588 modulating the delivery of curcumin, a natural molecule used as a model antioxidant  
589 compound. Our study showed that the fabrication of the composite is feasible and that the  
590 features of the two components can be successfully integrated. Stable films based on  
591 alginate and HELP were easily prepared establishing a protocol. FT-IR and thermal analysis  
592 evidenced an interaction between HELP and the carboxylate group of alginate, a  
593 phenomenon that is likely correlated to the final functional features of the material. The

594 presence of HELP in the composite was shown functional both to control the release of the  
595 model compound curcumin leading to a high antioxidant activity of the material and to  
596 maintain, and possibly enhance, the cytocompatibility of the final material. Overall, although  
597 further studies are needed to evaluate the in vivo behavior of this composite material,  
598 ourwork demonstrated that the association of alginate with HELP was effective to prepare  
599 customizable platforms for drug delivery, wound healing, and tissue regeneration. Finally, it  
600 worth noticing that HELP-based proteins are readily customizable by molecular fusion of  
601 exogenous domains to prepare active biopolymers. These HELP fusion proteins may  
602 represent in the future a further possibility to confer specific functionality to the final  
603 composite materials

604

## 605 **Author statement**

606 Carlo Bergonzi: Investigation, Visualization, Data curation, Writing - Original draft  
607 preparation; Giovanna Gomez d'Ayala: Investigation, Visualization, Data curation, Writing -  
608 Original draft preparation; Lisa Elviri: Supervision; Paola Laurienzo; Supervision,  
609 Methodology, Writing - Review & Editing; Antonella Bandiera; Supervision, Funding  
610 acquisition; Ovidio Catanzano: Investigation, Visualization, Methodology, Data  
611 curation, Writing - Review & Editing, Supervision.

612

## 613 **Declaration of competing interest**

614 The authors declared that there is no conflict of interest.

615

## 616 **Acknowledgement**

617 This work was funded by "Commissariato del Governo della Regione Friuli Venezia Giulia -  
618 Fondo Trieste" and managed by AREA Science park in the frame of "Made in Trieste"  
619 program. The authors are very grateful to Dr. Annalisa Bianchera for her precious help  
620 during cytotoxicity studies. The authors wish to thank Dr.M. Stebel for technical assistance  
621 in HELP polypeptide production and Prof. S. Passamonti for scientific assistance during the  
622 project.

623

## 624 **Appendix A. Supplementary data**

625 Supplementary data to this article can be found online at  
626 <https://doi.org/10.1016/j.ijbiomac.2020.07.084>.



628 **References**

- 629 [1] D. Akilbekova, M. Shaimerdenova, S. Adilov, D. Berillo, Biocompatible scaffolds based  
630 on natural polymers for regenerative medicine, *Int. J. Biol. Macromol.* 114 (2018) 324–333.
- 631 [2] A. Bianchera, O. Catanzano, J. Boateng, L. Elviri, The Place of Biomaterials in Wound  
632 Healing, *Therapeutic Dressings and Wound Healing Applications*, 2020 337–366.
- 633 [3] E. Salernitano, C. Migliaresi, Composite materials for biomedical applications: a review,  
634 *J Appl Biomater Biomech* 1 (1) (2003) 3–18.
- 635 [4] H. Semyari, M. Salehi, F. Taleghani, A. Ehterami, F. Bastami, T. Jalayer, H. Semyari, M.  
636 Hamed Nabavi, H. Semyari, Fabrication and characterization of collagenhydroxyapatite-  
637 based composite scaffolds containing doxycycline via freeze casting method for bone tissue  
638 engineering, *J. Biomater. Appl.* 33 (4) (2018) 501–513.
- 639 [5] J. Boateng, R. Burgos-Amador, O. Okeke, H. Pawar, Composite alginate and gelatin  
640 based bio-polymeric wafers containing silver sulfadiazine for wound healing, *Int. J. Biol.*  
641 *Macromol.* 79 (2015) 63–71.
- 642 [6] D. Zamani, F. Moztarzadeh, D. Bizari, Alginate-bioactive glass containing Zn and Mg  
643 composite scaffolds for bone tissue engineering, *Int. J. Biol. Macromol.* 137 (2019) 1256–  
644 1267.
- 645 [7] J. Venkatesan, I. Bhatnagar, P. Manivasagan, K.H. Kang, S.K. Kim, Alginate composites  
646 for bone tissue engineering: a review, *Int. J. Biol. Macromol.* 72 (2015) 269–281.
- 647 [8] R. Silva, R. Singh, B. Sarker, D.G. Papageorgiou, J.A. Juhasz-Bortuzzo, J.A. Roether, I.  
648 Cicha, J. Kaschta, D.W. Schubert, K. Chrissafis, R. Detsch, A.R. Boccaccini, Hydrogel  
649 matrices based on elastin and alginate for tissue engineering applications, *Int. J. Biol.*  
650 *Macromol.* 114 (2018) 614–625.
- 651 [9] J. Halper, M. Kjaer, Basic components of connective tissues and extracellular matrix:  
652 elastin, fibrillin, fibulins, fibrinogen, fibronectin, laminin, tenascins and thrombospondins, in:  
653 J. Halper (Ed.), *Progress in Heritable Soft Connective Tissue Diseases*, Springer  
654 Netherlands, Dordrecht 2014, pp. 31–47.
- 655 [10] F.W. Keeley, C.M. Bellingham, K.A. Woodhouse, Elastin as a self-organizing  
656 biomaterial: use of recombinantly expressed human elastin polypeptides as a model for  
657 investigations of structure and self-assembly of elastin, *Philos T R Soc B* 357 (1418) (2002)  
658 185–189.
- 659 [11] V. Groult, W. Hornebeck, P. Ferrari, J.M. Tixier, L. Robert, M.P. Jacob, Mechanisms of  
660 interaction between human skin fibroblasts and elastin - differences between elastin fibers  
661 and derived peptides, *Cell Biochem. Funct.* 9 (3) (1991) 171–182.
- 662 [12] S. Ito, S. Ishimaru, S.E. Wilson, Effect of coacervated alpha-elastin on proliferation of  
663 vascular smooth muscle and endothelial cells, *Angiology* 49 (4) (1998) 289–297.
- 664 [13] Q. Wen, S.M. Mithieux, A.S. Weiss, Elastin biomaterials in dermal repair, *Trends*  
665 *Biotechnol.* 38 (3) (2019) 280–291.

- 666 [14] W.F. Daamen, T. Hafmans, J.H. Veerkamp, T.H. van Kuppevelt, Comparison of five  
667 procedures for the purification of insoluble elastin, *Biomaterials* 22 (14) (2001) 1997–2005.
- 668 [15] D. Miranda-Nieves, E.L. Chaikof, Collagen and elastin biomaterials for the fabrication  
669 of engineered living tissues, *Acs Biomater Sci Eng* 3 (5) (2017) 694–711.
- 670 [16] G. Ciofani, G.G. Genchi, V. Mattoli, B. Mazzolai, A. Bandiera, The potential of  
671 recombinant human elastin-like polypeptides for drug delivery, *Expert Opin Drug Deliv* 11  
672 (10) (2014) 1507–1512.
- 673 [17] G. Ciofani, G.G. Genchi, P. Guardia, B. Mazzolai, V. Mattoli, A. Bandiera, Recombinant  
674 human elastin-like magnetic microparticles for drug delivery and targeting, *Macromol.*  
675 *Biosci.* 14 (5) (2014) 632–642.
- 676 [18] A. Bandiera, Transglutaminase-catalyzed preparation of human elastin-like  
677 polypeptide-based three-dimensional matrices for cell encapsulation, *Enzyme Microb Tech*  
678 49 (4) (2011) 347–352.
- 679 [19] P. D'Andrea, D. Civita, M. Cok, L.U. Severino, F. Vita, D. Scaini, L. Casalis, P. Lorenzon,  
680 I. Donati, A. Bandiera, Myoblast adhesion, proliferation and differentiation on human elastin-  
681 like polypeptide (HELP) hydrogels, *J Appl Biomater Func* 15 (1) (2017).
- 682 [20] P. D'Andrea, M. Sciancalepore, K. Veltruska, P. Lorenzon, A. Bandiera, Epidermal  
683 growth factor - based adhesion substrates elicit myoblast scattering, proliferation,  
684 differentiation and promote satellite cell myogenic activation, *Bba-Mol Cell Res* 1866 (3)  
685 (2019) 504–517.
- 686 [21] L. Corich, M. Buseti, V. Petix, S. Passamonti, A. Bandiera, Evaluation of a biomimetic  
687 3D substrate based on the Human Elastin-like Polypeptides (HELPS) model system for  
688 elastolytic activity detection, *J. Biotechnol.* 255 (2017) 57–65.
- 689 [22] A. Bandiera, A. Markulin, L. Corich, F. Vita, V. Borelli, Stimuli-induced release of  
690 compounds from elastin biomimetic matrix, *Biomacromolecules* 15 (1) (2014) 416–422.
- 691 [23] A. Bandiera, S. Passamonti, L.S. Dolci, M.L. Focarete, Composite of elastin-based  
692 matrix and electrospun poly(L-lactic acid) fibers: a potential smart drug delivery system,  
693 *Front Bioeng Biotech* 6 (2018).
- 694 [24] A. Bandiera, Elastin-like polypeptides: the power of design for smart cell encapsulation,  
695 *Expert Opin Drug Deliv* 14 (1) (2017) 37–48.
- 696 [25] A. Bandiera, Assembly and optimization of expression of synthetic genes derived from  
697 the human elastin repeated motif, *Prep Biochem Biotech* 40 (3) (2010) 198–212.
- 698 [26] A. Bandiera, P. Sist, R. Urbani, Comparison of thermal behavior of two recombinantly  
699 expressed human elastin-like polypeptides for cell culture applications, *Biomacromolecules*  
700 11 (12) (2010) 3256–3265.
- 701 [27] E.R. Morris, D.A. Rees, D. Thom, J. Boyd, Chiroptical and stoichiometric evidence of a  
702 specific, primary dimerisation process in alginate gelation, *Carbohydr. Res.* 66 (1) (1978)  
703 145–154.

- 704 [28] G.T. Grant, E.R. Morris, D.A. Rees, P.J.C. Smith, D. Thom, Biological interactions  
705 between polysaccharides and divalent cations: the egg-box model, *FEBS Lett.* 32 (1) (1973)  
706 195–198.
- 707 [29] R. Russo, M. Malinconico, G. Santagata, Effect of cross-linking with calcium ions on the  
708 physical properties of alginate films, *Biomacromolecules* 8 (10) (2007)3193–3197.
- 709 [30] J.S. Boateng, H.N. Stevens, G.M. Eccleston, A.D. Auffret, M.J. Humphrey, K.H.  
710 Matthews, Development and mechanical characterization of solvent-cast polymeric films as  
711 potential drug delivery systems to mucosal surfaces, *Drug Dev. Ind. Pharm.* 35 (8) (2009)  
712 986–996.
- 713 [31] J. Boateng, O. Catanzano, Advanced therapeutic dressings for effective wound  
714 healing—a review, *J. Pharm. Sci.* 104 (11) (2015) 3653–3680.
- 715 [32] J.S. Boateng, K.H. Matthews, H.N. Stevens, G.M. Eccleston, Wound healing dressings  
716 and drug delivery systems: a review, *J. Pharm. Sci.* 97 (8) (2008) 2892–2923.
- 717 [33] R. Russo, M. Abbate, M. Malinconico, G. Santagata, Effect of polyglycerol and the  
718 crosslinking on the physical properties of a blend alginate-hydroxyethylcellulose, *Carbohydr.*  
719 *Polym.* 82 (4) (2010) 1061–1067.
- 720 [34] G.B. Deacon, R.J. Phillips, Relationships between the carbon-oxygen stretching  
721 frequencies of carboxylate complexes and the type of carboxylate coordination, *Coord.*  
722 *Chem. Rev.* 33 (3) (1980) 227–250.
- 723 [35] P.R.K. Mohan, G. Sreelakshmi, C.V. Muraleedharan, R. Joseph, Water soluble  
724 complexes of curcumin with cyclodextrins: characterization by FT-Raman spectroscopy,  
725 *Vib. Spectrosc.* 62 (2012) 77–84.
- 726 [36] T.S. Pathak, J.S. Kim, S.-J. Lee, D.-J. Baek, K.-J. Paeng, Preparation of alginic acid  
727 and metal alginate from algae and their comparative study, *J. Polym. Environ.* 16 (3) (2008)  
728 198–204.
- 729 [37] M. Rezvanian, N. Ahmad, M.C.I. Mohd Amin, S.-F. Ng, Optimization, characterization,  
730 and in vitro assessment of alginate-pectin ionic cross-linked hydrogel film for wound  
731 dressing applications, *Int. J. Biol. Macromol.* 97 (2017) 131–140.
- 732 [38] A. Nešić, A. Onjia, S. Davidović, S. Dimitrijević, M.E. Errico, G. Santagata, M.  
733 Malinconico, Design of pectin-sodium alginate based films for potential healthcare  
734 application: study of chemico-physical interactions between the components of films and  
735 assessment of their antimicrobial activity, *Carbohydr. Polym.* 157 (2017) 981–990.
- 736 [39] M.R. Nobile, V. Pirozzi, E. Somma, G. Gomez D'Ayala, P. Laurienzo, Development and  
737 rheological investigation of novel alginate/N-succinylchitosan hydrogels, *J. Polym. Sci. B*  
738 *Polym. Phys.* 46 (12) (2008) 1167–1182.
- 739 [40] N.A. Peppas, P.A. Buri, Surface, interfacial and molecular aspects of polymer  
740 bioadhesion on soft tissues, *J. Control. Release* 2 (1985) 257–275.
- 741 [41] L.E. Tracy, R.A. Minasian, E.J. Caterson, Extracellular matrix and dermal fibroblast  
742 function in the healing wound, *Adv Wound Care (New Rochelle)* 5 (3) (2016) 119–136.



- 743 [42] International Standardization Organisation, ISO 10993-5 Biological Evaluation of  
744 Medical Devices, Part 5: Tests for Cytotoxicity, in Vitro Methods, Geneva, 1992.
- 745 [43] Y. Yuan, P. Korja, Proliferative activity of elastin-like-peptides depends on charge and  
746 phase transition, *J. Biomed. Mater. Res. A* 104 (3) (2016) 697–706.
- 747 [44] M. Schafer, S. Werner, Oxidative stress in normal and impaired wound repair,  
748 *Pharmacol. Res.* 58 (2) (2008) 165–171.
- 749 [45] B. D'Autreaux, M.B. Toledano, ROS as signalling molecules: mechanisms that generate  
750 specificity in ROS homeostasis, *Nat Rev Mol Cell Biol* 8 (10) (2007) 813–824.
- 751 [46] V.P. Menon, A.R. Sudheer, Antioxidant and anti-inflammatory properties of curcumin,  
752 in: B.B. Aggarwal, Y.-J. Surh, S. Shishodia (Eds.), *The Molecular Targets and Therapeutic*  
753 *Uses of Curcumin in Health and Disease*, Springer US, Boston, MA 2007, pp. 105–125.
- 754 [47] V.P. Menon, A.R. Sudheer, Antioxidant and anti-inflammatory properties of curcumin,  
755 *Adv. Exp. Med. Biol.* 595 (2007) 105–125.
- 756 [48] G.C. Jagetia, G.K. Rajanikant, Curcumin stimulates the antioxidant mechanisms in  
757 mouse skin exposed to fractionated gamma-irradiation, *Antioxidants (Basel)* 4 (1) (2015)  
758 25–41.
- 759 [49] S.D. Fitzmaurice, R.K. Sivamani, R.R. Isseroff, Antioxidant therapies for wound healing:  
760 a clinical guide to currently commercially available products, *Skin Pharmacol Phys* 24 (3)  
761 (2011) 113–126.
- 762 [50] A.M. Rasik, A. Shukla, Antioxidant status in delayed healing type of wounds, *Int. J. Exp.*  
763 *Pathol.* 81 (4) (2000) 257–263.
- 764
- 765

## Figures and tables

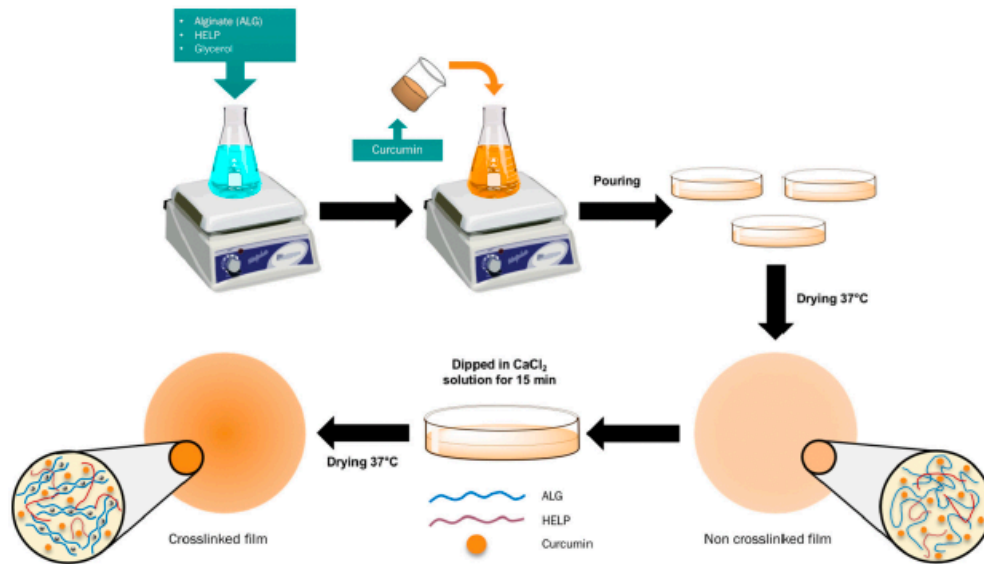


Fig. 1. Scheme of ALG/HELP composite film preparation.

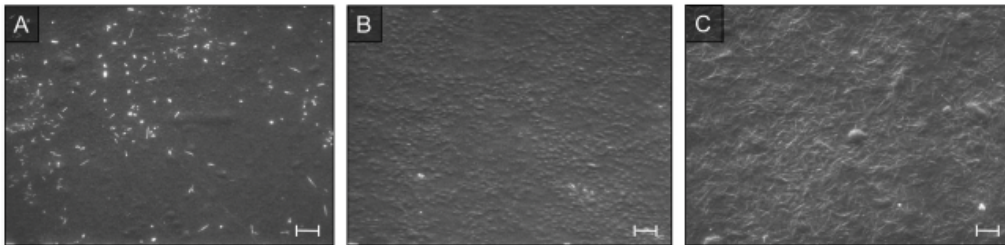
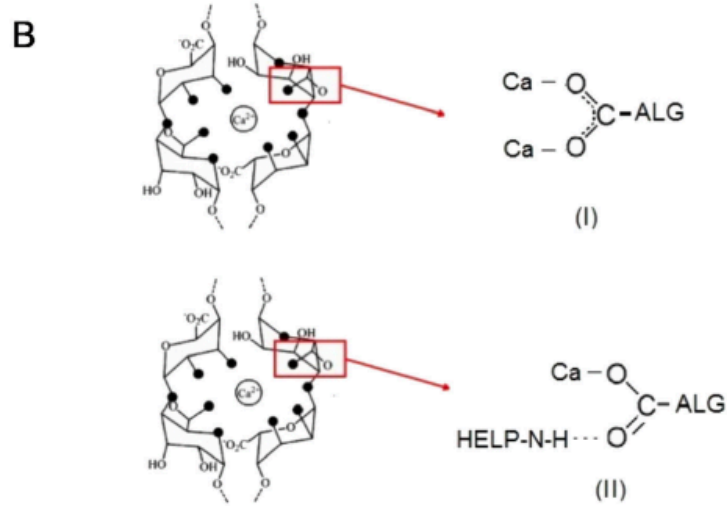
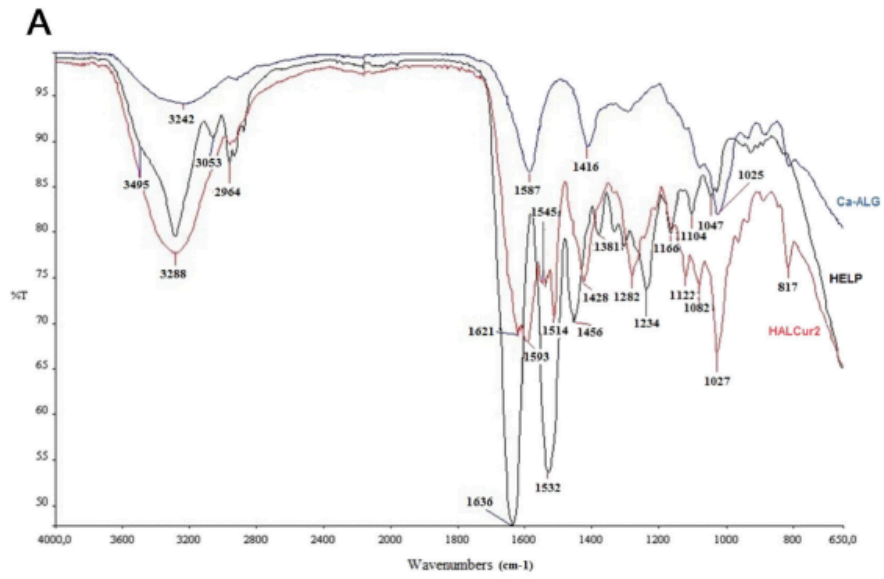
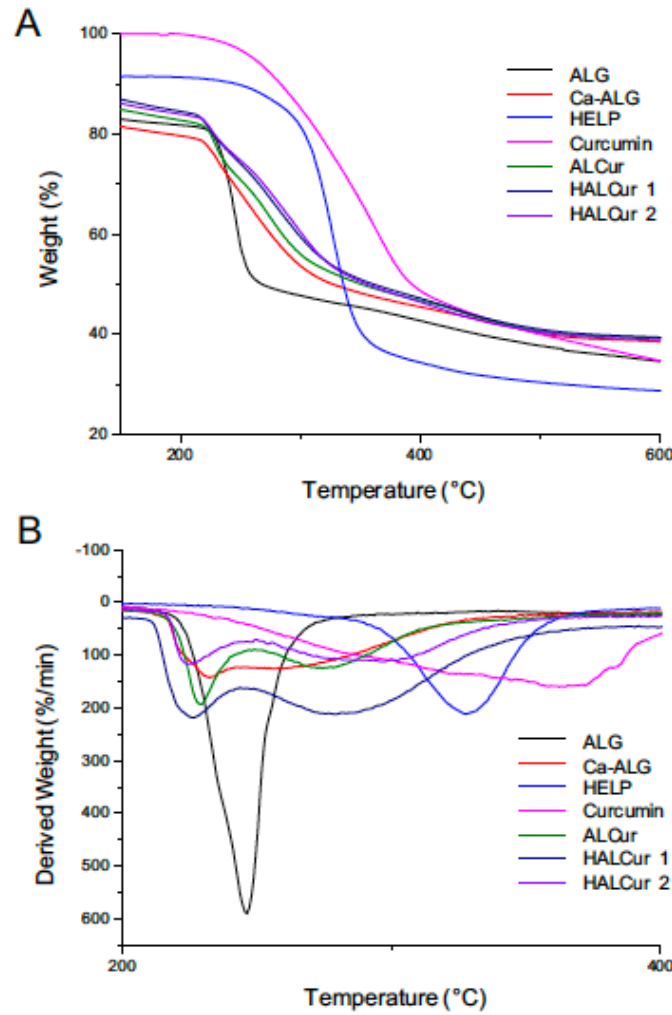


Fig. 2. SEM micrograph showing the surface topography of ALG/HELP films. A characteristic highly- $\alpha$  rugated surface structure with small and big wrinkles is formed with increasing HELP concentration. A) ALCur; B) HALCur 1; C) HALCur 2 (magnification 320 $\times$ ; scale bar = 20  $\mu$ m).



**Fig. 3.** A) FTIR spectra of HALCur 2, HELP and Ca-ALG. B) Egg-box structure of calcium alginate with the two different calcium-carboxylate coordination types: (I) bidentate bridging coordination (Ca-ALG); (II) bidentate pseudo-bridging coordination (HALCur 2).



**Fig. 4.** TGA (A) and DTG (B) curves of raw materials (ALG, HELP, and curcumin), crosslinked alginate film without curcumin (Ca-ALG), and ALCur, HALCur 1, and HALCur 2 films loaded with 0.1% curcumin.

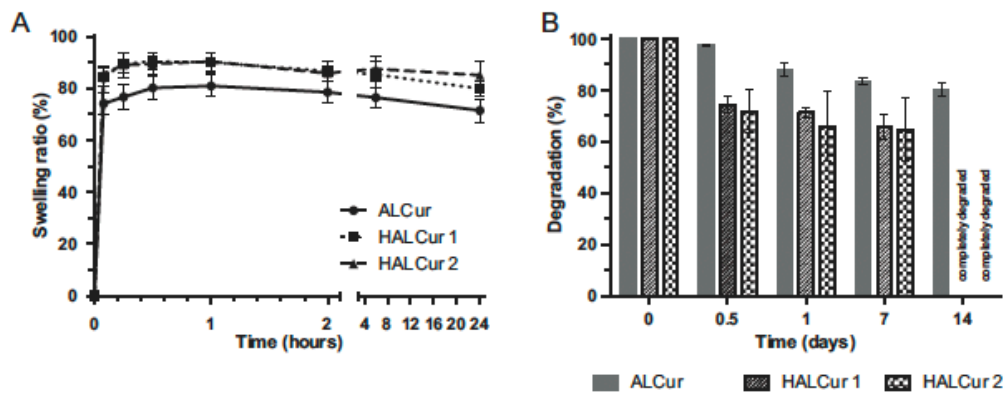


**Fig. 5.** Swelling (A) and stability (B) profiles of ALCur, HALCur 1, and HALCur 2 films loaded with 0.1% curcumin ( $n = 3, \pm SD$ ). After 24 h HALCur 1, and HALCur 2 films have a significantly ( $p < 0.05$ ) higher swelling capacity vs ALCur, while the difference between HALCur 1, and HALCur 2 was not significant. Similarly, the stability is related to the HELP presence, with the HALCur 1, and HALCur 2 films more susceptible to degradation after 14 days of immersion in PBS at 37 °C.

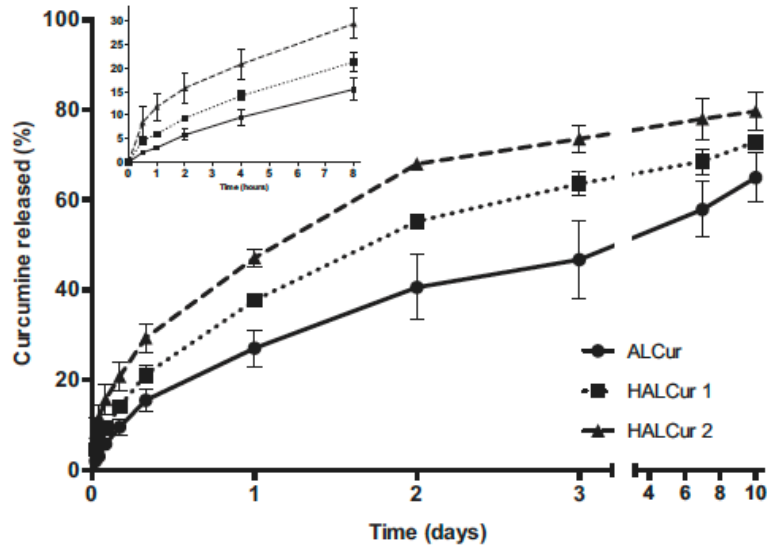


Fig. 6. Cumulative curcumin release (%) profiles from ALCur, HALCur 1, and HALCur 2 films. Results are reported as mean  $\pm$  standard deviation of three independent measurements. Lines through data points are to guide the eye.

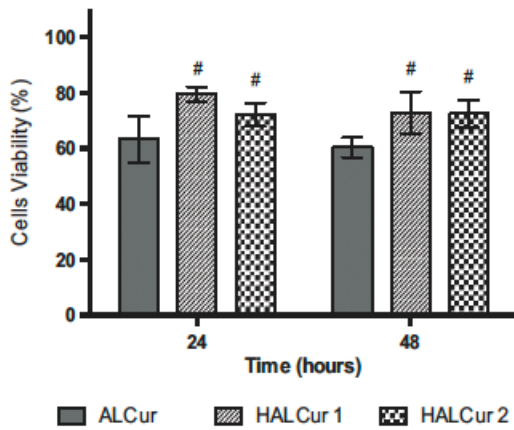


Fig. 7. Effect of ALG/HELP composite biomaterials on human dermal fibroblasts cells viability. Cell viability has been determined by resazurin assay. The results have been reported as percentage of viable cells compared with the control considered as 100% viable cells. Bars represent the mean  $\pm$  SD of triplicate determination in 3 independent experiments. # $p < 0.05$  vs. ALCur.

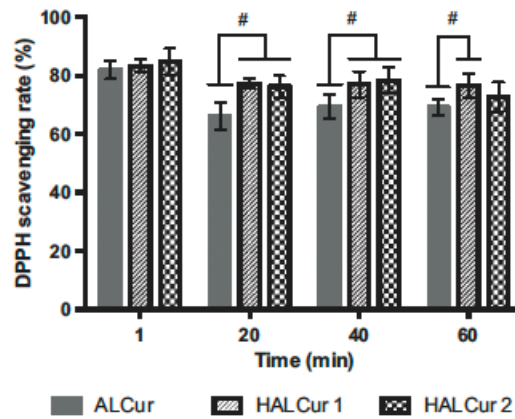


Fig. 8. *In vitro* antioxidant activity of the ALCur and HALCur films measured by the DPPH assay. Bars represent the mean  $\pm$  SD of triplicate determination in 3 independent experiments. # $p < 0.05$ .

Table 1

Thickness, Young modulus (E), elongation at break ( $\epsilon_{break}$ ) and max applied force  $\pm$  S.D. of films loaded with 0.1% curcumin.

Sample	Thickness ( $\mu\text{m}$ )	E (MPa)	$\epsilon_{break}$ (%)	Max Applied Force (N)
ALCur	5.7 $\pm$ 0.9	2398 $\pm$ 32	1.70 $\pm$ 0.34	10 $\pm$ 1
HALCur 1	5 $\pm$ 0.6	4074 $\pm$ 1249	1.10 $\pm$ 0.12	10 $\pm$ 1
HALCur 2	5.9 $\pm$ 1.3	5077 $\pm$ 845	0.80 $\pm$ 0.01	10 $\pm$ 1

**Table 2**

Thermal characteristics of the raw materials used to prepare the composite films, of the crosslinked alginate film without curcumin (Ca-ALG), and of the ALCur, HALCur 1, and HALCur 2 films loaded with 0.1% curcumin. The average relative error on DSC and TGA data is lower than 10%.

	T <sub>g</sub>	WL (%) up to 150 °C	T <sub>onset</sub> (°C)	T <sub>peak 1</sub> (°C)	T <sub>peak 2</sub> (°C)
HELP	-	8.7	208	328	
Curcumin	-	-	204	362	
ALG	n.d.	16.9	246	268	
Ca-ALG	104	20.4	211	232	256
ALCur	98	17.3	208	229	274
HALCur 1	109	15.5	210	226	278
HALCur 2	111	16.0	212	225	295